

Accurate Frequency Estimation with Fewer DFT Interpolations based on Padé Approximation

Kai Wu, J. Andrew Zhang, *Senior Member, IEEE*, Xiaojing Huang, *Senior Member, IEEE*, and Y. Jay Guo, *Fellow, IEEE*

Abstract—Frequency estimation is a fundamental problem in many areas. The well-known A&M and its variant estimators have established an estimation framework by iteratively interpolating the discrete Fourier transform (DFT) coefficients. In general, those estimators require two DFT interpolations per iteration, have uneven initial estimation performance against frequencies, and are incompetent for small sample numbers due to low-order approximations involved. Exploiting the iterative estimation framework of A&M, we unprecedentedly introduce the Padé approximation to frequency estimation, unveil some features about the updating function used for refining the estimation in each iteration, and develop a simple closed-form solution to solving the residual estimation error. Extensive simulation results are provided, validating the superiority of the new estimator over the state-the-art estimators in wide ranges of key parameters.

Index Terms—Frequency estimation; DFT; interpolation; Padé approximation; Cramér-Rao lower bound (CRLB).

I. INTRODUCTION

As a fundamental research issue, frequency estimation of a single-tone complex exponential signal has been investigated in many areas, including vehicular communication and sensing [1]–[3]. It is worth noting that vehicular radar/sensing based on communication waveforms is very popular currently [4], [5], where estimating target parameters can be treated as frequency estimation problems. Discrete Fourier transform (DFT) and its interpolation-based frequency estimation have attracted extensive attention, due to the low complexity and high efficiency. Earlier works exploit the fixed DFT coefficients, which can cause uneven estimation bias for different frequencies [2]. In [6], the authors introduced an iterative DFT-interpolated frequency estimator, known as A&M, which improves the asymptotic mean squared error (MSE) performance to 1.0147 times the Cramér-Rao lower bound (CRLB). Many variants of A&M have been developed, achieving various improvements, e.g., a more accurate initial estimate [7], a smaller estimation bias [8], a particular treatment of real sinusoidal signals [9], and an improved asymptotic performance [10].

A common issue of the above estimators [6]–[10] is that each iteration requires at least $2N$ complex multiplications, with N denoting the number of signal samples. This complexity is scaled up with the number of iterations. The issue is specifically treated in [7] which proposes an improved initial estimate that can reduce up to two interpolations yet with the same asymptotic performance as the original A&M. The issue is also noticed in [10] which uses the same number of interpolations as A&M but achieves a better asymptotic performance.

K. Wu, J. A. Zhang, Xiaojing Huang and Y. J. Guo are with the Global Big Data Technologies Centre, University of Technology Sydney, Sydney, NSW 2007, Australia (e-mail: kai.wu@uts.edu.au; andrew.zhang@uts.edu.au; xiaojing.huang@uts.edu.au; jay.guo@uts.edu.au).

Another common issue of the estimators [6]–[10] is that a first-order Taylor series (TS) is used for approximating the relation between the *updating function* and the estimation error¹. On one hand, this makes the estimators incompetent for small N 's, since the first-order TS is only valid for large N 's. On the other hand, the large approximation error can lead to uneven estimation accuracy for different frequencies. As a consequence, more iterations may be required for a satisfactory estimate [10]. We underline that the small- N scenario is not uncommon. The frequency estimator studied here can be used for estimating the angle-of-arrival (AoA) [11], [12], which is known as *spatial frequency*, of an antenna array. The number of antennas available for the spatial DFT is practically limited.

This correspondence is motivated to improve the estimation accuracy of the DFT interpolation-based frequency estimator, reduce interpolations and enhance the applicability to wider range of sample numbers. A key innovation of this work is unprecedentedly introducing the Padé approximation (PA) to the interpolation-based frequency estimation. PA employs the ratio of two polynomials to approximate a given power series, e.g., TS, where the sum of the degrees of the two polynomials in a PA is equal to the degree of the power series [13, Sec. 5.12]. Underlying the successful application of PA are several key contributions, as summarized below.

We construct the PA that approximates the sixth-order TS of the updating function (in contrast to the first-order TS employed in most previous designs [6]–[10]). We prove some useful features of the updating function in terms of its monotonicity and symmetry, and use the features to simplify the PA by suppressing some high-order terms. We also derive the coefficients of the simplified PA. Moreover, we develop a closed-form solution to solving the frequency estimation error from the established PA, where we apply the features of the updating function to remove the ambiguities in the solution. Extensive simulations validate that our estimator achieves more uniform performance across wide ranges of sample numbers and frequencies, and approaches CRLB more tightly, compared with state-of-the-art estimators.

II. SIGNAL MODEL

Consider the estimation of the unknown frequency f from the following N samples of a complex single-tone exponential signal,

$$s(n) = Ae^{j\left(\frac{2\pi fn}{f_s} + \phi\right)} + z(n), \quad n = 0, 1, \dots, N-1, \quad (1)$$

¹As will be illustrated in Section III-A, the updating function is used for calculating the estimation error in each iteration.

where A , f_s , ϕ and N denote the signal amplitude, the sampling rate, the initial phase and the sample number, respectively. The additive white Gaussian noise (AWGN) is denoted by $z(n)$. The frequency f can be decomposed into the sum of an integer and a fractional multiples of f_s/N , i.e.,

$$f = (k^* + \delta)f_s/N, \quad \delta \in [-0.5, 0.5], \quad (2)$$

where k^* denotes an integer and δ a non-integer. Taking the N -point DFT of $s(n)$, i.e., $\sum_{n=0}^{N-1} s(n)e^{-j\frac{2\pi kn}{N}}$, yields,

$$S(k) = \sum_{n=0}^{N-1} \tilde{A}e^{j\frac{2\pi(k^*+\delta)n}{N}}e^{-j\frac{2\pi kn}{N}} + Z(k), \quad (3)$$

where $\tilde{A} = Ae^{j\phi}$, f in (1) is replaced by its expression given in (2), and $Z(k)$ denotes the DFT of $z(n)$. The integer k^* can be estimated by identifying the maximum of $|S(k)|^2$, i.e.,

$$k^* : \max_{k \in [0, N-1]} |S(k)|^2. \quad (4)$$

As generally treated in previous works [6]–[10], we assume that k^* is accurately estimated so as to focus on refining the frequency estimate by estimating δ . This is a legitimate assumption, since we tend to focus on the asymptotic performance of a frequency estimator, as achieved in high SNR regions, when developing a new estimator or comparing with the previous ones. Also following the related works [6]–[10], we focus on the single-tone signal to introduce the new ideas/designs. The extension to multi-tone scenarios will be remarked in Section V.

III. PROPOSED FREQUENCY ESTIMATOR

In this section, a new estimator is developed to iteratively estimate δ . We first introduce the core updating function, based on which we establish the overall estimator.

A. Core Updating Function

Consider the i -th iteration, where the estimate of δ from the previous iteration, as denoted by δ_{i-1} , is available. With reference to [10], we interpolate the DFT coefficients at

$$k_{i,\pm} = k^* + \delta_{i-1} \pm q_i, \quad (5)$$

where k^* is given in (2), and q_i is an extra controlling parameter used to shift the interpolation positions. Plugging $k = k_{i,\pm}$ into (3), the interpolated DFT coefficients are

$$S(k_{i,\pm}) = \tilde{A}\sin(\pi(\xi_i \mp q_i))/\sin(\pi(\xi_i \mp q_i)/N), \quad (6)$$

where $\tilde{A} = \tilde{A}e^{j\frac{(N-1)\pi}{N}(\xi_i \mp q_i)}$, \tilde{A} given in (3), $\xi_i (= \delta - \delta_{i-1})$ denotes the estimation error in the $(i-1)$ -th iteration, and the noise term is dropped for brevity. Denoting $S_{i,\pm} = S(k_{i,\pm})$, we can construct the following ratio,

$$\rho_i = (|S_{i,+}|^2 - |S_{i,-}|^2) / (|S_{i,+}|^2 + |S_{i,-}|^2) \quad (7)$$

The purpose of doing so is to estimate ξ_i from ρ_i . Let $\hat{\xi}_i$ denote the estimate of ξ_i . We can use $\hat{\xi}_i$ to refine the δ estimation as follows [6], [10],

$$\delta_i = \delta_{i-1} + \hat{\xi}_i, \quad \text{s.t. } \hat{\xi}_i \approx \xi_i = \delta - \delta_{i-1}. \quad (8)$$

Next, we illustrate how to estimate $\hat{\xi}_i$ from ρ_i .

Introducing the function $\mathcal{S}(\xi_i, \pm q_i) = \frac{\sin^2(\pi(\xi_i \mp q_i))}{\sin^2(\pi(\xi_i \mp q_i)/N)}$, the right-hand side (RHS) of (7) can be written into

$$f(\xi_i) = \frac{\mathcal{S}(\xi_i, q_i) - \mathcal{S}(\xi_i, -q_i)}{\mathcal{S}(\xi_i, q_i) + \mathcal{S}(\xi_i, -q_i)}. \quad (9)$$

Jointly observing (7) and (9), we see that estimating $\hat{\xi}_i$ from ρ_i is equivalent to solving the equation $f(\xi_i) = \rho_i$. Some features of $f(\xi_i)$, which are useful for deriving the solution, are provided in the following lemma; refer to Appendix A for its proof.

Lemma 1: For $|\xi_i| \leq q_i$, $f(\xi_i)$ monotonically increases with ξ_i , and presents odd symmetry around the origin, i.e., $f(-\xi_i) = -f(\xi_i)$.

From (9), we see that it can be difficult to directly solve the equation $f(\xi_i) = \rho_i$, due to the existence of the squared sine functions. To simplify the equation, many previous estimators, e.g., [6]–[10], [14], use the first-order TS of $f(\xi_i)$ which is valid for large N 's. In contrast, we propose to use the PA to approximate the following TS of $f(\xi_i)$ (of degree six), i.e.,

$$\tilde{f}(\xi_i) = \sum_{l=0}^6 c_l \xi_i^l = c_1 \xi_i + c_3 \xi_i^3 + c_5 \xi_i^5, \quad (10)$$

where the even powers of ξ_i are suppressed since $f(\xi_i)$ is an odd function of ξ_i , as illustrated in Lemma 1. We propose to use the following PA to approximate the above TS,

$$\hat{f}(\xi_i) = \left(\sum_{p=0}^P a_p \xi_i^p \right) / \left(\sum_{r=0}^R b_r \xi_i^r \right), \quad P = R = 3, \quad (11)$$

$$\text{s.t. } \hat{f}(0) = \tilde{f}(0); \quad \hat{f}^{(k)}(0) = \tilde{f}^{(k)}(0), \quad k = 1, \dots, P + R,$$

where $h^{(k)}(x)$ denotes the k -th derivative of $h(x)$ (h can be \hat{f} or \tilde{f}) and $h^{(k)}(0)$ is value of $h^{(k)}(x)$ at $x = 0$. Note that the rationale for setting $P = R = 3$ is illustrated in Appendix B.

Also note that the constraints in (11) constitute $(P + R + 1)$ equations, which can be used to express the coefficients of the PA, i.e., a_p and b_r , in terms of those of TS, i.e., c_l . We underline that the properties of $f(\xi_i)$ unveiled in Lemma 1 can be used to suppress some high-order terms in $\hat{f}(\xi_i)$. As illustrated in Appendix B, we have $a_0 = a_2 = 0$ and $b_1 = b_3 = 0$. Plugging these constraints into the $(P + R + 1)$ equations, the PA coefficients can be solved, with the following solution achieved.

Lemma 2: The function $f(\xi_i)$ can be approximated by $\hat{f}(\xi_i)$ with the approximation error in the order of $\mathcal{O}(\xi_i^7)$, where

$$\hat{f}(\xi_i) = (a_1 \xi_i + a_3 \xi_i^3) / (1 + b_2 \xi_i^2),$$

$$\text{with } a_1 = c_1, a_3 = c_3 - c_1 c_5 / c_3, b_2 = c_5 / c_3. \quad (12)$$

Equating $\hat{f}(\xi_i)$ obtained in Lemma 2 to ρ_i calculated in (7), we obtain that $a_1 \xi_i + a_3 \xi_i^3 = \rho(1 + b_2 \xi_i^2)$, which can be further turned into a cubic equation of ξ_i ,

$$\xi_i^3 + k_2 \xi_i^2 + k_1 \xi_i + k_0 = 0,$$

$$\text{s.t. } k_2 = -\rho b_2 / a_3, k_1 = a_1 / a_3, k_0 = -\rho / a_3, \quad (13)$$

Using the cubic formula [15], the three roots of the above equation can be given by

$$\begin{aligned} z_1 &= -k_2/3 + 2B, \quad z_2 = -k_2/3 - B + D, \\ z_3 &= -k_2/3 - B - D, \end{aligned} \quad (14)$$

where $B = (S + T)/2$ and $D = \sqrt{3}(S - T)j/2$; $S = \sqrt[3]{R + \sqrt{D}}$ and $T = \sqrt[3]{R - \sqrt{D}}$; $D = Q^3 + R^2$, $R = (9k_1k_2 - 27k_0 - 2k_2^3)/54$ and $Q = (3k_1 - k_2^2)/9$; and k_0, k_1 and k_2 are given in (13). To determine the final estimate of ξ_i , we provide the following.

Lemma 3: *The estimate of ξ_i is given by*

$$\hat{\xi}_i = z_{i^*}, \text{ s.t. } i^* = \operatorname{argmin}_i |z_i|. \quad (15)$$

Proof: As proved in Lemma 1, $f(\xi_i)$ is monotonic against ξ_i for $|\xi_i| < q_i$. Thus, we can only have one solution to $f(\xi_i) = \rho_i$ in the region of $|\xi_i| < q_i$. Since the continuous region covers $\xi_i = 0$ (the smallest value that can be taken), the solution to the equation $\hat{f}(\xi_i) = \rho_i$ in the region is the smallest root given in (14). This leads to the (15). ■

Based on the above analyses and derivations, we summarize below the steps of estimating δ_i from δ_{i-1} .

Algorithm 1: *Given $a_1, a_3, b_2, \delta_{i-1}$ from iteration $(i - 1)$ and q_i , and provided that $|\xi_i| \leq q_i$, δ_i can be estimated as follows:*

- 1) Interpolate the DFT coefficients at $k_{i,\pm}$ given in (5), leading to $S_{i,\pm}$ given in (7);
- 2) Construct ρ_i , as illustrated in (7);
- 3) Compute the coefficients k_0, k_1 and k_2 based on (13);
- 4) Compute the three roots in (14);
- 5) Obtain the estimate of ξ_i , as given in Lemma 3;
- 6) Update δ_i as done in (8).

B. Initialization and Proposed Estimator in Overall

As revealed in [10], a high-quality initialization can speed up the asymptotic convergence of an iterative frequency estimator. Below, we provide a high-quality initialization of the proposed estimator with a single interpolation; c.f., two or more interpolations in many previous designs [6]–[10], [14].

Assume that $\delta \in [0, 0.5]$ holds. If we set $\delta_0 = 0.25$, then the estimation error ξ_1 satisfies that $\xi_1 = \delta - \delta_0 \in [-0.25, 0.25]$. Accordingly, we can set $q_1 = 0.25$ and run Algorithm 1 to estimate δ_1 . Moreover, we notice that $\delta_0 - q_1 = 0$. This indicates that one of the interpolated DFT coefficients is at $k_{1,-} = k^* + \delta_0 - q_1 = k^*$. This DFT coefficient has been computed when identifying k^* ; see (4) in Section II. Thus, we only need to interpolate one DFT coefficient at $k_{1,+} = k^* + \delta_0 + q_1 = 0.5$. The above analysis also applies for the case of $\delta \in [-0.5, 0]$. Then, the next question is how to determine the initial region of δ . To do so, the following sign test [7] can be performed by reusing the DFT results for identifying k^* ,

$$\alpha = \operatorname{sign}\{[S(k^* - 1) - S(k^* + 1)]S^\dagger(k^*)\}, \quad (16)$$

where k^* is given in (2), and $()^\dagger$ takes the complex conjugate. Using α , we have

$$\delta \in [0, 0.5], \text{ if } \alpha > 0; \text{ or } \delta \in [-0.5, 0], \text{ if } \alpha < 0. \quad (17)$$

As will be illustrated in Section IV, the sign test has a high accuracy in the sense that the estimators with or without using the sign test approach the CRLB from the same SNR.

Based on the above initialization and Algorithm 1, we summarize the overall processing of the proposed frequency estimator in the following algorithm.

Algorithm 2: *Input: $N, \delta_0 = 0.25\alpha, q_1 = 0.25, q_i$ ($i = 2, \dots, I$), the coefficient set $\mathcal{C}_1 = \{a_1, a_3, b_2\}$ for δ_1 , and the sets $\mathcal{C}_i = \{a_1^{(i)}, a_3^{(i)}, b_2^{(i)}\}$ for δ_i ($i \geq 2$). The proposed estimator performs as follows:*

- 1) Estimate δ_1 by running Algorithm 1 once based on N, δ_0, q_1 and \mathcal{C}_1 ;
- 2) For each $i = 2, \dots, I$, run Algorithm 1 iteratively based on N, δ_{i-1}, q_i and \mathcal{C}_i .

The final frequency estimate is given by $\hat{f} = \frac{f_s(k^* + \hat{\delta}_I)}{N}$.

We remark that, it is non-trivial to analyze the (asymptotic) performance of the proposed estimator. The main reason is because the analysis strategy, as developed in [14] and widely used in previous works [6]–[10], relies on a linear approximation between ρ_i and ξ_i ; whereas, in contrast, we use the non-linear PA to pursue a high-accuracy depiction of the relation between the two variables. Nevertheless, through extensive simulations to be provided in Section IV, our estimator is seen to outperform several state-of-the-art estimators which have the theoretical guarantee of approaching the CRLB. Two other remarks on Algorithm 2 are provided below.

1) *Computational Complexity (CC):* To analyze the overall CC of the proposed estimator, we first evaluate the CC of Algorithm 1. Its CC is dominated by that of interpolating DFT coefficients in Step 1). According to (3), one interpolation needs N complex multiplications (CMs). As illustrated above (16), a single interpolation is required for the first iteration, while for iteration $i (\geq 2)$, we need $2N$ CMs to interpolate the DFT coefficients twice. Algorithm 2 runs Algorithm 1 for I times, and thus its overall CC is dominated by $N + (I - 1) \cdot 2N = (2I - 1)N$ CMs. In contrast, the CC of the previous estimators, e.g., the three benchmarks to be illustrated in Section IV-A, are dominated by $2IN$ CMs. As will be illustrated in Section IV, the proposed estimator is able to approach the CRLB after only two iterations, i.e., $I = 2$.

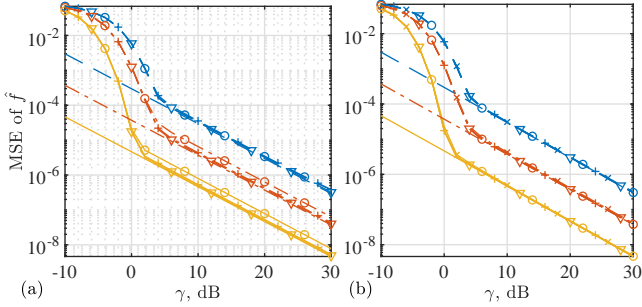
2) *Selection of q_i :* We recommend taking $q_i = q_1 = 0.25$ ($\forall i$) given two reasons. *First*, the proposed estimator is robust against the value of q_i , or in other words the estimation performance remains almost the same across a wide range of q_i 's. This will be illustrated in Fig. 5 of Section IV. *Second*, a benefit of taking of $q_i = q_1 = 0.25$ ($\forall i$) is that only one set of PA coefficients, i.e., \mathcal{C}_1 , are required to be stored onboard, saving storage and time for indexing different sets (if used) in practical systems.

IV. SIMULATION RESULTS

In this section, we provide simulation results to validate the superior performance of the proposed estimator over the previous estimators.

TABLE I: Marker and Line Style Definitions in Simulation Results.

Marker	o	+	×	▽	none
Estimator	AM	GAM	HAQSE	Proposed	CRLB
Line style	dash		dash-dotted	solid	
N	8		16	32	

Fig. 1: MSE of \hat{f} versus γ : (a) is for the first iteration, (b) for the second.

A. Benchmark Estimators

Several related estimators are simulated as benchmarks which can be implemented in the framework of Algorithm 2. Below, we only highlight their differences from our estimator.

1) *A&M* [6]: This estimator always interpolates the DFT coefficients at $k_{i,\pm} = k^* + \delta_{i-1} \pm 0.5$ ($\forall i \geq 1$) with $\delta_0 = 0$ taken. The ratio $\rho_i = \frac{|S(k_{i,+})| - |S(k_{i,-})|}{|S(k_{i,+})| + |S(k_{i,-})|}$ is constructed in each iteration, and $\xi_i = \rho_i/2$. A&M also has a different construction of ρ_i which leads to the same asymptotic performance as the one given above and hence is not considered here.

2) *Generalized A&M (GAM)* [7]: This estimator iterates as A&M but starts from a different initial δ_0 . In particular, GAM takes $\delta_0 = \alpha\beta$, where α is given in (16) and $\beta = 0, 0.25$ and 0.5 are considered and compared in the work. Here, for a fair comparison with our estimator, we only consider $\beta = 0.25$.

3) *Hybrid A&M and q-Shift Estimator (HAQSE)* [10]: This estimator applies A&M for δ_1 . Then, starting from $i = 2$, HAQSE interpolates the DFT coefficients at $k_{i,\pm} = k^* + \delta_{i-1} \pm q_H$, where $q_H = N^{-1/3}$ is proven to be sufficient for the estimator to converge to the CRLB for large N 's and $q_H \leq 0.32$ is suggested in [3] to ensure the validity of HAQSE also for small N 's. HAQSE constructs ρ_i as $\rho_i = \Re \left\{ \frac{S(k_{i,+}) - S(k_{i,-})}{S(k_{i,+}) + S(k_{i,-})} \right\}$ and updates $\xi_i = \frac{q_H \cos^2(\pi q_H)}{1 - \pi q_H \cot(\pi q_H)} \rho_i$.

B. Results and Analysis

Unless otherwise specified, the following parameters are used for all the estimators: $k^* = 2$, $f_s = 1$, $I = 2$, $\delta \in \mathcal{U}_{[-0.5, 0.5]}$, $q_1 = q_2 = 0.25$ (for the proposed estimator), and $q_H = N^{-1/3}$ (for HAQSE). Note that $\mathcal{U}_{[-0.5, 0.5]}$ denotes the uniform distribution in $[-0.5, 0.5]$. All the results to be presented are averaged over 5×10^4 independent trials. Moreover, the CRLB [6], given by $\frac{6f_s^2}{4\pi^2\gamma N^3}$, is provided in most simulation results, where $\gamma = \frac{|A|^2}{\sigma_0^2}$ is the SNR of the single-tone signal given in (1), and σ_0^2 denotes the noise variance of $z(n)$ therein. As interpreted in Table I, different estimators in the simulation results are differentiated by markers, while different values of N are distinguished by line styles.

Fig. 1 plots the MSE of \hat{f} against γ , where $N = 8, 16$ and 32 are simulated. We see that the MSEs of \hat{f} converge

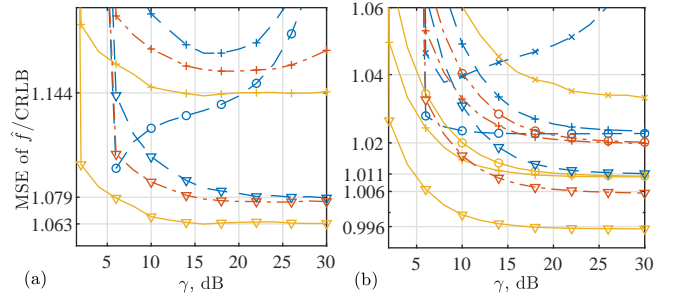
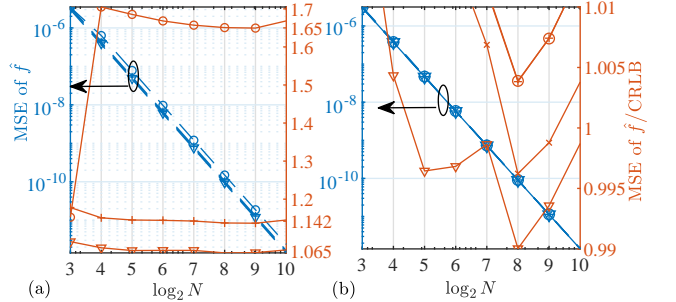


Fig. 2: Illustration of the ratio between MSE and CRLB to better compare different estimators: (a) for the first iteration, (b) for the second. For better clarity, range limits are imposed on the y-axes, and hence the estimators with larger MSEs become invisible in the figure.

Fig. 3: MSE performance against N , where $\gamma = 20$ dB, (a) for the first iteration, and (b) for the second.

to the CRLB for all the estimators. Comparing the two sub-figures, it is obvious that the estimation performance of all the estimators is further improved (closer to the CRLB) after the second iteration. Fig. 2 zooms in the differences among the estimators by normalizing the MSEs plotted in Fig. 1 against their respective CRLBs. We see from Fig. 2(a) that, after the first iteration, the proposed estimator already achieves the MSE as low as 1.079 times the CRLB for a small $N = 8$, and reduces the MSE to 1.063 times the CRLB for $N = 32$, which is notably based on a single interpolation. We see from Fig. 2(b) that, after the second iteration, the proposed estimator persistently outperforms the benchmark estimators across the whole region of γ and approaches the CRLB more tightly.

We see from Fig. 2(b) that the simulated MSE can be smaller than the CRLB, yet with a considerably small difference. Two reasons may cause this phenomenon. *First*, CRLB is derived for a deterministic parameter that is under estimation, while the frequency taken for the simulations is random over independent trials. We remark that this random configuration is necessary for a fair comparison of different estimators, since they can have dramatically distinct estimation performance over frequencies, as will be illustrated in Fig. 4. *Second*, this phenomenon can be caused by the finite number of independent (Monte-Carlo) trials. Refer to [10, Sec. V] for a detailed analysis of this aspect.

Fig. 3 illustrates the MSE performance w.r.t. N . From Fig. 3(a), we see that, after the first iteration, the normalized MSEs of the proposed estimator is as low as 1.065 which is improved by about 6.74% over A&M and GAM (both achieve the minimum about 1.142). We also see that the proposed estimator present a more stable asymptotic performance than A&M and GAM, as N increases. From Fig. 3(b), we see that,

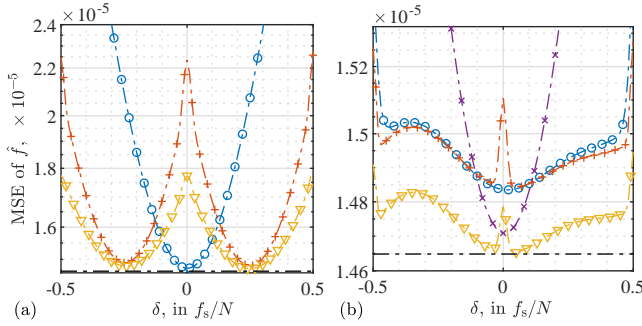


Fig. 4: MSE performance versus δ , where (a) for the first iteration, and (b) for the second. Note that $N = 16$, $\gamma = 20$ dB, and 100 discrete values are evenly taken in the region of $\delta \in [-0.5, 0.5]$.

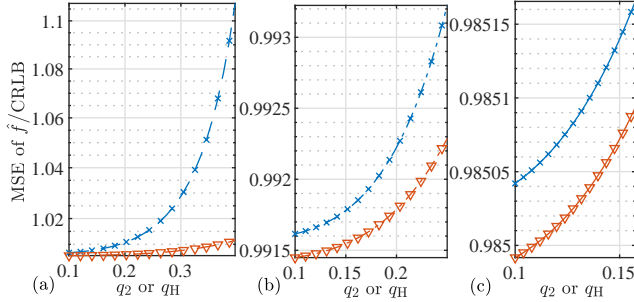


Fig. 5: MSE performance versus q_2 , where $\gamma = 20$ dB. The sub-figures (a), (b) and (c) are for $N = 8, 16$ and 32 , respectively. For fair comparison with HAQSE, we set $q_H = q_2$ which is evenly taken from $[0.1, N^{-1/3}]$.

after the second iteration, the proposed estimator is able to approach the CRLB for almost all values of N , while HAQSE can only achieve this for large N 's. This is expected since HAQSE is designed for large N 's. On the other hand, this highlights the benefit of introducing the Padé approximation.

Fig. 4 plots the MSE of different estimators against the whole region $\delta \in [-0.5, 0.5]$. We see from Fig. 4(a) that the proposed estimator already has a close-to-CRLB performance at some δ after the first iteration. We also see that the proposed estimator provides a performance lower bound for GAM. This is expected, since both estimators take $\delta_0 = 0.25$ while the proposed one achieves a more accurate approximation between ρ_i and ξ_i . We see from Fig. 4(b) that, after the second iteration, the proposed estimator achieves the best flatness in the whole region of δ .

Fig. 5 compares HAQSE and the proposed estimator in terms of q_2 (for the proposed) or q_H (for HAQSE). We see that both estimators show the tight convergence to the CRLB in the case of $N = 16$ and 32 , and show the robustness against q . This is consistent with the analysis in [10] that the asymptotic performance of HAQSE shall remain the same for $q_H \leq N^{-1/3}$. We also see that our estimators always provides a performance lower bound for the HAQSE across the whole region of q_2 . Notably, we see that, for the small $N = 8$, our estimator still presents a stable MSE performance over q_2 's, while HAQSE shows an increasingly worse performance as q_H increases. The visible improvement achieved by the proposed estimator over the state-of-the-art HAQSE is: *on one hand*, due to the more accurate initial estimate in the first iteration, as has been demonstrated in Figs. 1 to 4; and *on the other hand*, ensured by the newly proposed much more accurate approximation between ρ_i and ξ_i .

V. CONCLUSION AND REMARKS

This correspondence develops an accurate frequency estimator with fewer interpolations yet better accuracy and wider applicability to small number of samples, as compared with the state-of-the-art estimators. This is achieved by introducing, for the first time, the Padé approximation in approximating the updating function of estimation error. This is also accomplished by newly unveiled features of the updating function and the derivation of a closed-form solution to solving the residual estimation error in each iteration. Extensive simulations validate the performance superiority of the proposed estimator over the state-of-the-art estimators.

We remark that the single-tone scenario is focused on in this correspondence for introducing the new ideas. Using the estimate-and-subtract strategy² (ESS) [11], [16], [17], a single-tone estimator can often be extended to multi-tone scenarios. For instance, the two benchmarks A&M [6] and HAQSE [10], originally developed for single tone, have been successfully applied to multi-tone scenarios applying ESS [11], [16], [17]. The proposed estimator, combining ESS, is expected to work for multi-tone scenarios as well, since it outperforms A&M and HAQSE, as presented in Section IV. The detailed extension is deferred to future work.

APPENDIX

A. Proof of Lemma 1

Since $0 < q_i \leq 0.5$ is satisfied, $\mathcal{S}(\xi_i, \pm q_i)$ approximates the square of a sinc function [18]. Hence, we know that $\mathcal{S}(\xi_i, q_i)$ is a monotonically increasing function from $-q_i$ to q_i while $\mathcal{S}(\xi_i, -q_i)$ monotonically decreases in the same region. These can be translated into $\mathcal{S}'_+ > 0$, $\mathcal{S}'_- < 0$, where \mathcal{S}'_+ denotes the first derivative of $\mathcal{S}(\xi_i, q_i)$ w.r.t. ξ_i and \mathcal{S}'_- is similarly defined for $\mathcal{S}(\xi_i, -q_i)$. Accordingly, the monotonicity of $f(\xi_i)$ can be deduced from its first derivative, i.e., $f' = 2(\mathcal{S}'_+ \mathcal{S}_- - \mathcal{S}'_- \mathcal{S}_+) / [\mathcal{S}_+ + \mathcal{S}_-]^2 > 0$, where \mathcal{S}_+ denotes $\mathcal{S}(\xi_i, q_i)$, and \mathcal{S}_- denotes $\mathcal{S}(\xi_i, -q_i)$.

From the expression given in (9), we know that $\mathcal{S}(\xi_i, \pm q_i)$ is symmetric about $\xi_i = \pm q_i$. Thus, they are also symmetric about the axis of $\xi_i = 0$ in the region of $|\xi_i| \leq q_i$, i.e.,

$$\mathcal{S}(\xi_i, q_i) = \mathcal{S}(-\xi_i, -q_i), \quad \mathcal{S}(-\xi_i, q_i) = \mathcal{S}(\xi_i, -q_i). \quad (18)$$

Applying this symmetry in (9) leads to

$$\begin{aligned} f(-\xi_i) &= \frac{\mathcal{S}(-\xi_i, q_i) - \mathcal{S}(-\xi_i, -q_i)}{\mathcal{S}(-\xi_i, q_i) + \mathcal{S}(-\xi_i, -q_i)} \\ &= \frac{\mathcal{S}(\xi_i, -q_i) - \mathcal{S}(\xi_i, q_i)}{\mathcal{S}(\xi_i, q_i) + \mathcal{S}(\xi_i, -q_i)} = -f(\xi_i), \end{aligned}$$

which shows the symmetry of $f(\xi_i)$ about the origin.

²The strategy first estimates each frequency coarsely as a single tone, as if there were no other tones; then, from the second round, each tone is refined by subtracting the recovered signals of other tones. With more rounds of refinement performed, the estimates of all tones can be increasingly accurate.

B. Rationale of Setting $(P, R) = (3, 3)$

Based on (10), the TS $\tilde{f}(\xi_i)$ is of degree six. Thus, according to [13, Sec. 5.12], we have $P + R = 6$ for the PA $\hat{f}(\xi_i)$ given in (11). Lemma 1 shows $f(0) = 0$. Solving $\hat{f}(0) = 0$ yields $a_0 = 0$, which then indicates $P \geq 1$. Lemma 1 also states $f(-\xi_i) = -f(\xi_i)$. To preserve the odd symmetry, the numerator and denominator of $\hat{f}(\xi_i)$ can only have odd and even powers of ξ_i , respectively, since there is a non-zero constant b_0 in the denominator. Based on the above analysis, $(P, R) = (1, 5)$ or $(2, 4)$ leads to the same PA with the degree of the denominator polynomial up to four; $(P, R) = (3, 3)$ or $(4, 2)$ leads to the same PA with the degree of the denominator polynomial up to three; and $(P, R) = (5, 1)$ or $(6, 0)$ makes the PA degenerated into TS. Given that a cubic polynomial can be more tractable than a quartic one, we employ the PA with $(P, R) = (3, 3)$.

REFERENCES

- [1] W. Wang *et al.*, "Near optimal timing and frequency offset estimation for 5G integrated LEO satellite communication system," *IEEE Access*, vol. 7, pp. 113 298–113 310, 2019.
- [2] E. Aboutanios, "Frequency estimation for low earth orbit satellites," Ph.D. dissertation, Faculty of Engineering (Telecommunications Group), UTS, 2002.
- [3] K. Wu, W. Ni, J. Andrew Zhang, R. P. Liu, and Y. Jay Guo, "Refinement of optimal interpolation factor for DFT interpolated frequency estimator," *IEEE Commun. Lett.*, vol. 24, no. 4, pp. 782–786, 2020.
- [4] R. C. Daniels, E. R. Yeh, and R. W. Heath, "Forward collision vehicular radar with IEEE 802.11: Feasibility demonstration through measurements," *IEEE Trans. Veh. Techn.*, vol. 67, no. 2, pp. 1404–1416, 2018.
- [5] J. A. Zhang, X. Huang, Y. J. Guo, J. Yuan, and R. W. Heath, "Multibeam for joint communication and radar sensing using steerable analog antenna arrays," *IEEE Trans. Veh. Techn.*, vol. 68, no. 1, pp. 671–685, 2019.
- [6] E. Aboutanios and B. Mulgrew, "Iterative frequency estimation by interpolation on Fourier coefficients," *IEEE Trans. Signal Process.*, vol. 53, no. 4, pp. 1237–1242, April 2005.
- [7] Y. Liu, Z. Nie, Z. Zhao, and Q. H. Liu, "Generalization of iterative Fourier interpolation algorithms for single frequency estimation," *Digital Signal Process.*, vol. 21, no. 1, pp. 141–149, 2011.
- [8] J.-R. Liao and C.-M. Chen, "Phase correction of discrete Fourier transform coefficients to reduce frequency estimation bias of single tone complex sinusoid," *Signal Process.*, vol. 94, pp. 108 – 117, 2014.
- [9] S. Ye, J. Sun, and E. Aboutanios, "On the estimation of the parameters of a real sinusoid in noise," *IEEE Signal Process. Lett.*, vol. 24, no. 5, pp. 638–642, May 2017.
- [10] A. Serbes, "Fast and efficient sinusoidal frequency estimation by using the DFT coefficients," *IEEE Trans. Commun.*, vol. 67, no. 3, pp. 2333–2342, March 2019.
- [11] E. Aboutanios, A. Hassanien, M. G. Amin, and A. M. Zoubir, "Fast iterative interpolated beamforming for accurate single-snapshot DOA estimation," *IEEE Geosci. Remote Sens. Lett.*, vol. 14, no. 4, pp. 574–578, 2017.
- [12] K. Wu, J. Andrew Zhang, X. Huang, Y. Jay Guo, and R. W. Heath, "Waveform design and accurate channel estimation for frequency-hopping MIMO radar-based communications," *IEEE Trans. Commun.*, pp. 1–1, 2020.
- [13] W. H. Press, S. A. Teukolsky, W. T. Vetterling, and B. P. Flannery, *Numerical recipes 3rd edition: The art of scientific computing*. Cambridge university press, 2007.
- [14] B. G. Quinn, "Estimating frequency by interpolation using Fourier coefficients," *IEEE trans. Signal Process.*, vol. 42, no. 5, pp. 1264–1268, 1994.
- [15] E. W. Weisstein, "Cubic formula," <https://mathworld.wolfram.com/>, 2002.
- [16] S. Ye and E. Aboutanios, "Rapid accurate frequency estimation of multiple resolved exponentials in noise," *Signal Process.*, vol. 132, pp. 29–39, 2017.
- [17] A. Serbes and K. Qaraqe, "A fast method for estimating frequencies of multiple sinusoids," *IEEE Signal Process. Lett.*, vol. 27, pp. 386–390, 2020.
- [18] A. V. Oppenheim, J. R. Buck, and R. W. Schaffer, *Discrete-time signal processing. Vol. 2*. Upper Saddle River, NJ: Prentice Hall, 2001.